Thermodynamic Analysis of Distributed Propulsion

Galen J. Suppes* and Adam B. Suppes†
HS-Drone, LLC, Charlottesville, VA 22911

The ability of propulsion Sources (Sources) to increase the L/D-efficiency of aircraft is highly dependent on the Sources' locations, surrounding surface morphologies, and lost work associated with Sources' operating points. Computational fluid dynamics (CFD) calculations were performed on airfoils (i.e., 2D CFD) to provide guidelines for identifying base case specifications of these variables. Trailing-edge upper-surface Source locations provided the greatest direct impact on L/D-efficiency, but mid-chord Sources provided the ability to minimize the interference of sequential thin-plate wing sections. Optimal surrounding surface morphologies depend on the mode of operation, being different for descent and cruising; and so, morphing surfaces are needed to maximize the effectiveness of distributed propulsion. Relative to free stream conditions, Sources have lower pressures at intakes and higher pressures at discharges; the optimal positioning of these pressure differences to generate lift has a significant impact on L/D-efficiency. Metrics were identified to maximize the gain-loss ratio of increased L/D-efficiency versus lost thrust. Distributed-propulsion approaches have particular utility toward designing high-*L/D* low-*AR* airframes.

Nomenclature

2D = two dimensional.

3D = three Dimensional

AR = aspect ratio, defined as the span divided by a representative longitudinal chord length

Camber = curvature of an airfoil characterized as a deviation from straight as a either a fraction of the chord length or percent of a chord length (e.g., 0.01 c or 1%)

* Chief Engineer, Homeland Technologies, LLC, gjsuppes@gmail.com
† Senior Research Engineer, Homeland Technologies, LLC

C_d = drag coefficient

CFD = computational fluid dynamics

c, Chord = chord, distance from leading edge to trailing edge of an airfoil or wing

C_l = lift coefficient

Curl = a favorable flow of air from below the leading edge to the upper surface resulting in a low pressure area on the upper surface immediately behind the leading edge.

D = drag, form drag is due to pressure on the surface, total drag as equal to sum of form and shear drag

L/D = lift-drag ratio, the primary measure of airframe efficiency

lift pressures = pressures that generate aerodynamic lift such as lower pressures on upper surfaces and higher pressures on lower surfaces.

Loss = lost energy term of Bernoulli equation (J/kg)

P = pressure (N/m^2) pressure is absolute pressure unless a subscript of G identifies gauge pressure with reference as free stream pressure, 1 atm

Source = a Source of propulsion, a Source generates thrust

u = velocity of air relative to an airframe

t/c = thickness to chord ratio, thickness is a maximum vertical dimension

VTOL = vertical takeoff and landing

α_P = angle from horizontal (°), subscript P identifies angle of a point on a line or surface

ρ = density (kg/m^3), typically density of air

Introduction

THE interference of surfaces near an aircraft's propulsor (Source) is inevitable, but good design provides a greater gain in aircraft L/D-efficiency from improved surface pressure profiles than loss in thrust from the interference. Particularly for low aspect ratio (AR) aircraft and thin-cambered airfoils, the beneficial pressure gradients of distributed propulsion can be extended over larger surfaces and ultimately compensate for much of the side-edge air flows that reduce L/D efficiency. In the burgeoning applications of solar power, the nexus of low AR designs, thin-plate cambered airfoils, and solar power is able to provide more-robust and higher-speed solar aircraft.

CFD simulations enable rapid progress on understanding effective use of distributed propulsion. While the ability to qualitatively and quantitatively relate pressure profiles to L/D is a standard outcome of CFD simulations, quick metrics to quantify the impact surface interferences on Source thrust are not yet standard analyses. Energy balances and lost work analyses are able to fill the void of easy-to-use metrics. This paper progresses from CFD analysis, to analysis of gain-loss rations, and finally to a heuristic-level summaries of the findings.

Background

A high ***L/D*** for an airfoil (i.e., cross sections of a wing or lifting body) is a necessary, but not sufficient, condition for a high ***L/D*** on a wing based on that airfoil. Air flow around side edges dissipates lift forces into the surrounding free stream. While thin-plate cambered airfoils have significant advantages toward next-generation solar aircraft, side-edge losses are particularly high and solutions to this issue are needed.

Thin-plate cambered airfoils have unique features toward ultra-light wing sections and bifacial solar panels. Above clouds and snow-covered ground, bifacial panels can more than double the productivity of panels at Earth's surface without greenfield or brownfield construction costs.

Previous works emphasized elevating the understanding of thin-plate airfoils to heuristics, Table 1, which assist in rapid specification of base case designs. [1, 2] The current work emphasizes the advancement of methods and understanding towards the use of Sources to achieve high L/D low AR aircraft.

Table 1. Heuristics on designing to create aerodynamic lift and flight efficiency. Copied with permission from HS-Drone, LLC. (ref. TRB Paper)

For Airfoils (2D cross-sections):

- **A-1.** Air's velocity impacting a surface generates higher Pressure.
- **A-2.** Air's velocity diverging from a surface generates lower Pressure.
- **A-3.** Air expands at speed of sound from high-to-low Pressure (except within boundary layer).
- **A-4.** Air's velocity bends toward lower Pressure and away from higher Pressure.
- **A-5.** A surface's L/D is the normalized surface integral of Pressure $\tan^{-1}(\alpha)$ on the surface, per:

$$Lift = \Delta P\, \Delta S\, Cos(\alpha_P); \quad Drag_{form} = \Delta P\, \Delta S\, Sin(\alpha_P);$$

$$L/D = \frac{1}{Tan(\alpha_P)} = \frac{57}{\alpha_P^\circ} \; at\ low\ \alpha_P \qquad \text{(Equation A-5)}$$

- **A-6.** Shear forces are negligible at $C_d > 0.01$; $C_{d,\,shear} < 0.001$ for smooth surface.

For the addition of Sources (Propulsion, i.e. jets, propellers, etc.):

- **S-1.** Increasing Source power increases Lift at trailing edge of Lift Spans; Lift Span pitch angles < 1° from horizontal increase L/D as limited by Operating Point. The term "Lift Span" is used to define the surface area impacted by a Source's low pressure intake.
- **S-2.** For L/D > 40, induced thrust is necessary; induced thrust counteracts Drag.
- **S-3.** For the highest L/D: the Lift Span, Nose, and (optional) wings need to have pitches coordinated with Lift Span interaction with a Source.
- **S-4.** High induced Drag on surfaces > 3° should be eliminated by transforming pressure to near free stream pressures or transforming surface through addition of induced thrust.
- **S-5.** A mid-chord Source can propagate lower pressure forward to increase overall L/D.
- **S-6.** Optimal Lift Span pitches decrease with increasing Source power.

For Wings (i.e. 3D airfoils):

- **W-1.** Lift pressures are lost over side edges for a wing relative to an airfoil.
- **W-2.** Use camber, fences, and distributed Sources to compensate for lost Lift pressure.
- **W-3.** High AR wings may be added to low AR lifting bodies to increase L/D.
- **W-4.** Wing loadings vary with application, approximately: Military jets (700 kg/m^2, with C_L of 1.5), commercial jets (300-500, 1.5-1.6), commercial prop aircraft (100-200, 0.8), prop drones (50, 0.5)C, and HAPS/HALE (2-7, <0.4). When essentially all the planform generates lift, $C_L = [m\ g] / [\rho\ A\ u^2]$. Where at a planform loading 2, $C_L = 2\ g / [\rho\ u^2]$. At 80 m/s and 0.1 kg/m^3 $C_L = 0.03$ (i.e., HAPS aircraft have much lower C_L than jets).

Equation 1, referred hereafter as "the ***AR Equation***," is a lifting line theory [3-5] relation between lift, drag, and AR for a wing without mitigation of side-edge losses.

$$C_d = \frac{c_l^2}{\pi AR\, e} \qquad (1)$$

where C_d is the drag coefficient, C_l is the lift coefficient, and e is an efficiency factor. Equation 1 provides a benchmark for progress to overcome side-edge losses.

Side-edge lift loss mitigation is an important part of wing design. Wings of elliptical planform and sword point

ends were early methods to mitigate side-edge losses. Contemporary airliners often incorporate winglets to mitigate side-edge losses. Winglets typically form vertical surfaces parallel to free stream velocity and can extend over eight feet high, which is 13.3% of a 120 ft wingspan. With decreasing ***AR***, the winglets (i.e., fences) do not scale well, creating unacceptably high (e.g., >50% of the wingspan) weight and drag. This paper pursues identifying more-optimal fence heights and geometries for use with high-chord side edges of low AR wing.

Related Work – CFD simulations have been repeatedly validated toward accurately characterizing airfoils and basic wing structures. [6][7][8][9-12] The CFD simulations of this work are discussed in terms of fundamental physical phenomena consistent with the results, which provides additional reinforcement of result validity.

Achieving high L/D in a wing's airfoil cross section is a necessary, but not sufficient, condition to achieve high L/D. Previous work on thin-plate cambered airfoils identify: attainable L/D of 135, a theoretical basis to attain values up to 155, and ability to use learning algorithms to optimize base case designs toward these high L/D. [13][14][15][16]

Distributed propulsion has been identified as being able to reduce emissions per passenger mile by 50% and reduce fuel burns by 70%.[9, 10][17] The review by Gohardani dates distributed propulsion to 1924, including 20 different design milestones.[18] Reviews of distributed propulsion identify approaches along: a) wingtip Sources, b) midspan (and root) wing Sources, and c) lifting-body trailing-edge Sources. [13][14][15]

Trailing-edge distributed propulsion on upper surfaces of lifting bodies is a common approach identified by several reviews. Pascual investigated more-novel aspects on a flying wing, with an emphasis on the impact of engine position on aerodynamic interference. [19] Pascual identified preferred locations behind the airframe's trailing edge as having minimum installation interference losses; this finding is discussed in the Discussion section of this paper.

Wingtip propulsors have been identified as effective to increase L/D, especially effective were wingtip propellers turning in a direction opposite that of a wing vortex. The vortex loss is an extreme side-edge loss Source due to flow from lower surfaces to upper surfaces as the surfaces separated by a thin wing and have pressures that significantly deviate from free stream pressures. Multiple papers verify these findings. (Site) Sinnige et al identify that use of propulsion on wingtips decreased drag, swirl, and inboard up-rotation. [20-24] Other papers identify the vertical location of the propeller as impacting the efficacy of wingtip propellers; and under certain circumstances, a propeller near the root of the wing out-performs wingtip propellers. [21, 25] In particular, wingtip pusher configurations can reduce L/D. [26] Heuristics can eliminate some disadvantageous designs, such as wingtip tractor configurations, early

in the design process. [26]

One category of applications that benefit from instant work are wings with long-chord side edges which are absent classical wingtip shapes. An example application is a rectangular towed platform with an aspect ratio between 0.2 and 1.0. Optimal approaches to distributed propulsion on long-chord side edges, such as along the sides of a towed platform, are different than on wingtips.

Wing-based distributed propulsion are reported on contemporary wing designs with maximum t/c > 0.04[27] [28] Instant paper places an emphasis on thin cambered airfoils with having t/c < 0.015, the resulting thin wings have different challenges and opportunities.

Benchmark, Control, and Base Case

Analysis and interpretations of Source performances from CFD is meaningful primarily in the context of proper benchmarks, controls, and base cases.

Benchmarks are representative approaches to which new approaches can be compared. In subsonic aerodynamics, higher-pressure air expands in all directions, unless blocked by a surface, and will repel approaching free stream air. Thus, no matter how a Source is mounted to an airframe, there will be interference. And so, the absolute performance of a Source is less pertinent than performance relative to benchmark configuration.

In CFD simulation of thrust for a Source, energy input is put into the fluid as a pressure increase which can be estimated from CFD simulation results per Equation 2 as applied to a tight control volume around the Source. A larger control volume that extends to surface and free stream conditions yields Equation 3 which has Loss of thrust as a variable.

$$\left(\frac{P_G}{\rho}\right)_{Sout} - \left(\frac{P_G}{\rho}\right)_{Sin} \approx E_{Source} \tag{2}$$

$$\left(\frac{U^2}{2}\right)_{Sout} + \left(\frac{P_G}{\rho}\right)_{Sout} - x_{BL}\left(\frac{U^2}{2}\right)_{BL} - x_{BL}\left(\frac{P_G}{\rho}\right)_{BL} - (1 - x_{BL})\left(\frac{U^2}{2}\right)_{FS} + Loss = E_{Source} \tag{3}$$

where $\boldsymbol{P}$ is pressure, $\boldsymbol{u}$ is longitudinal velocity, $\boldsymbol{\rho}$ is density, $\boldsymbol{x_{BL}}$ is mass flow rate through the Source volume with the Source turned off divided by the flow rate with the Source at the specified power setting, $\boldsymbol{E}$ is the energy input to the Source, and $\boldsymbol{FS}$ refers to free stream conditions. Example loss are non-longitudinal velocities and heat from shear losses along a duct surface.

Controls are necessary to estimate the thrust generated by a power setting. Typically, the control is the control volume around a Source with the Source inactive. The control takes into account velocity and pressure gradients

created by the structure to which the Source is attached.

In these studies, the base case is an airfoil with a Source that achieves a goal, such as increasing ***L/D***. The base case identifies process viability. The base case is often a starting point for designed experiments toward identifying optimal configurations and modes of operation.

Experimental Methods

Simflow software was used to perform CFD calculations of lift, drag, pressure profiles, and velocity profiles for STL files of a Source in the proximity of objects of interest. Objects of interest include thin-plate airfoils, ducts, and lifting bodies. Typical scales were airfoils 1 m in length and Sources 1 to 5 mm in height and 0.1 to 0.5 mm thick. Most simulations were 2D with a few illustrative 3D simulations. Simflow directly calculated lift and drag coefficients as a function of free stream velocity and simulation conditions.

Vertical slices of the pressure and velocity profiles were exported to MS Excel from Paraview software at about 1 mm in front of the leading edge of the Source and 1 mm behind the trailing edge of the Source. Control conditions, including respective boundary layer profiles, were taken at the leading edge of the Source with the Source turned off. Numerical integration was performed using MS Excel software to calculate velocity-averaged pressure and velocity thus allowing explicit solution for Loss and Source power as a function of Simflow Source settings. The equation derivations are in the Supplemental material of this document and summarized in Table 4 in the Discussion section.

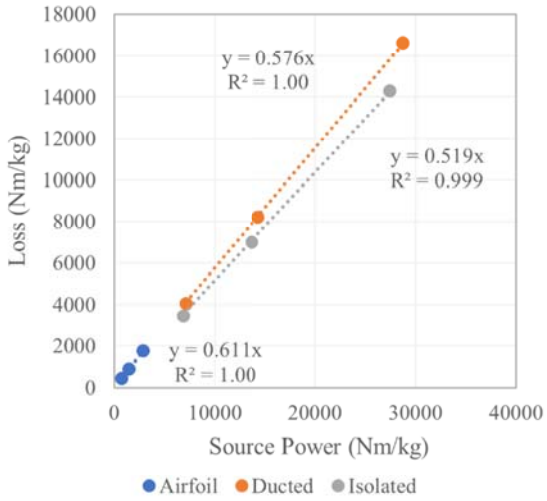

Fig. 1 Example correlation of loss with Source based on analysis of pressure and velocity profiles around the Source per Equations 2 and 3.

Figure 1 illustrates an observed nearly linear dependence of Loss to Source power setting (units of m^2/s^2). Linear

regression estimates the Loss from a case study Source and surface (e.g., a thin plate airfoil) versus a benchmark Source with surface (e.g., a ducted airfoil) and independent Source (e.g. Source separated from any structure). Values of Loss, Source power, Drag, and Lift as a function of Source setting allowed numerical estimation of $\left(\frac{\partial D}{\partial [Loss]}\right)_{Lift}$. Numerical integration of this partial derivative allows for cumulative values of Drag reduction versus Source to be estimated (i.e., gain-loss analysis).

CDF results are at a constant pitch configuration versus the constant lift constraint of the differential equation. In practice, a wing's pitch is often adjusted (i.e., a flap or aircraft pitch is adjusted) to keep lift constant as velocity changes. Equation 4 was used to adjust Drag to meet the constant lift constraint.

$$Drag_{adj} = Drag * \frac{Lift_{ref}}{Lift} \qquad (4)$$

where $Lift_{ref}$ is the reference lift for maintaining the constant in the partial derivative.

The Loss as calculated previously this may be converted to the force acting upon the airfoil through Equation 5:

$$F_{Loss} = Loss * \rho * H * W \qquad (5)$$

where H is the height of the Source term and W is the width. Equation 5 provides the total force loss from the Source term.

Results

Flat Plate - Comparison of Source Locations

Screening studies were performed on Sources over a range of locations on a flat plate airfoil at α_A. = 0°. Absent Sources, the plate had 0 ***L/D*** with a horizontally symmetric pressure profile. The Source tends to create lower pressures on surfaces before the Source and higher pressures on surfaces aft the airfoil; the following three Source locations were evaluated:

- A leading-edge Source beneath the leading edge created lift pressures below the leading edge, but it also created reverse lift pressures above the leading edge (left, Figure 2). The intake pulls in air from afore and above the leading edge. The respective downward component of the velocity vector spreads to adjacent air which impacts the upper leading-edge surface. That impacting air creates the undesirable higher pressures. The higher pressures on the upper surface impact the pressure profile throughout the airfoil surface and make this Source ineffective to increase ***L/D***.
- An upper surface mid-chord Source creates lower pressures fore (advantage) and higher pressures

aft (disadvantage) the Source (middle, Figure 2). Moderate increases in ***L/D*** are observed due to the introduction of a favorable curl of airflow at the leading edge (hereafter, "curl"). If the Source were on the lower surface, a horizontally flipped pressure profile results with a decrease in ***L/D***.

- An upper surface trailing-edge Source (right, Figure 2) produces desirable increases in lift pressure throughout the airfoil, including formation of a favorable curl and lift pressures at the leading edge with sufficient power. A horizontally or vertically flipped version of this combination would create negative lift forces.

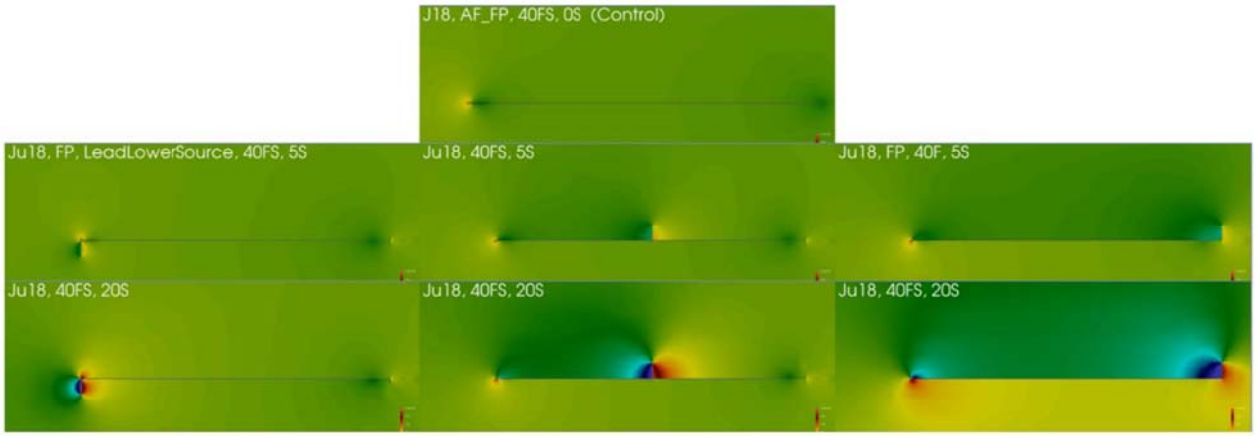

Fig. 2. Use of Sources at three locations with two power settings each on a flat plate airfoil at 0° α_P.

The conclusion is that upper-surface trailing-edge Sources can create the highest ***L/D***. Heuristic A-5 identifies the need to place lift pressures at $-1° < \alpha_P < 1°$ to incrementally increase L/D at values above 57. To achieve high L/D, the Source should be placed on a trailing-edge upper surface with $-1° < \alpha_P < 1°$. By example, if the intake of the Source is on a surface of $\alpha_P = 10°$ the incremental impact of the Source would be a lift of 5.7, with 1 part form drag for 5.7 parts lift.

While Fig. 2 directly illustrates Sources in three locations, its' pressure profiles can be extended to six locations due to flat airfoil symmetry. Heuristics S-1 and S-5 summarize these findings.

Further studies elucidate impacts of camber and use of both mid-chord and trailing-edge Sources. Figure 3 provides representative pressure profiles for a mid-section Source with trailing Sources. The airfoil sections have a portion of the mid-chord Source between the leading airfoil section and the trailing airfoil section. The Figure 3 airfoils reveal:

- A convex upward camber can improve the performance of the mid-chord Source since discharged air diverges slightly form the surface to reduce the magnitude of the higher-pressure region aft the Source.
- As stronger trailing Sources are used in addition to the mid-section Source, the trailing Source is sufficient to create the leading-edge curl; the advantages of the mid-chord Source diminish with the higher power setting of the trailing-edge Source.

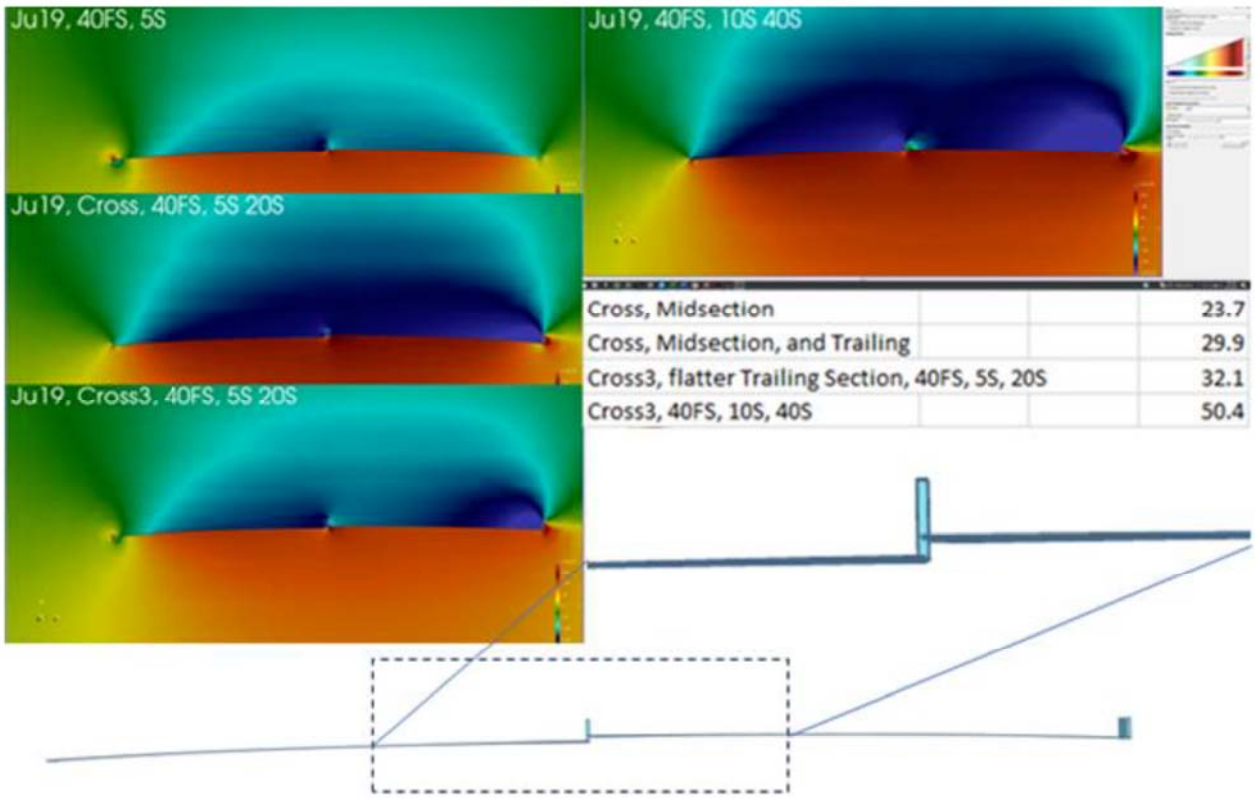

Fig. 3. Illustration of preferred mid-chord Source with representative pressure profiles and performance. The Source extends above the leading edge of the trailing airfoil subsection. L/D values are provided in the table.

A mid-chord Source also impacts aspects of performance that can mitigate side losses; the investigation of side-edge loss mitigation is outside the scope of this paper.

Part of the discharge of the Fig. 3 mid-chord Source flows under the leading edge of the trailing airfoil section. The thinner the trailing/leading edges interfacing with a mid-chord Source, the better the mid-chord Source performance (per additional CFD results, not shown). A mid-chord crossover Source is primarily effective with thin-plate cambered airfoils. Ideally, the leading-edge of the trailing airfoil section is knife-sharp to minimize the higher-

pressure air formation by the mid-section leading edge.

The leading airfoil sections of Fig. 3 airfoils have an $\alpha_A \approx -1°$ to garner the advantages of induced thrust. The trailing airfoil sections have an $\alpha_A \approx 1°$. Fig. 4 provides separate pressure profiles for the isolated leading and trailing airfoils of Fig. 3.

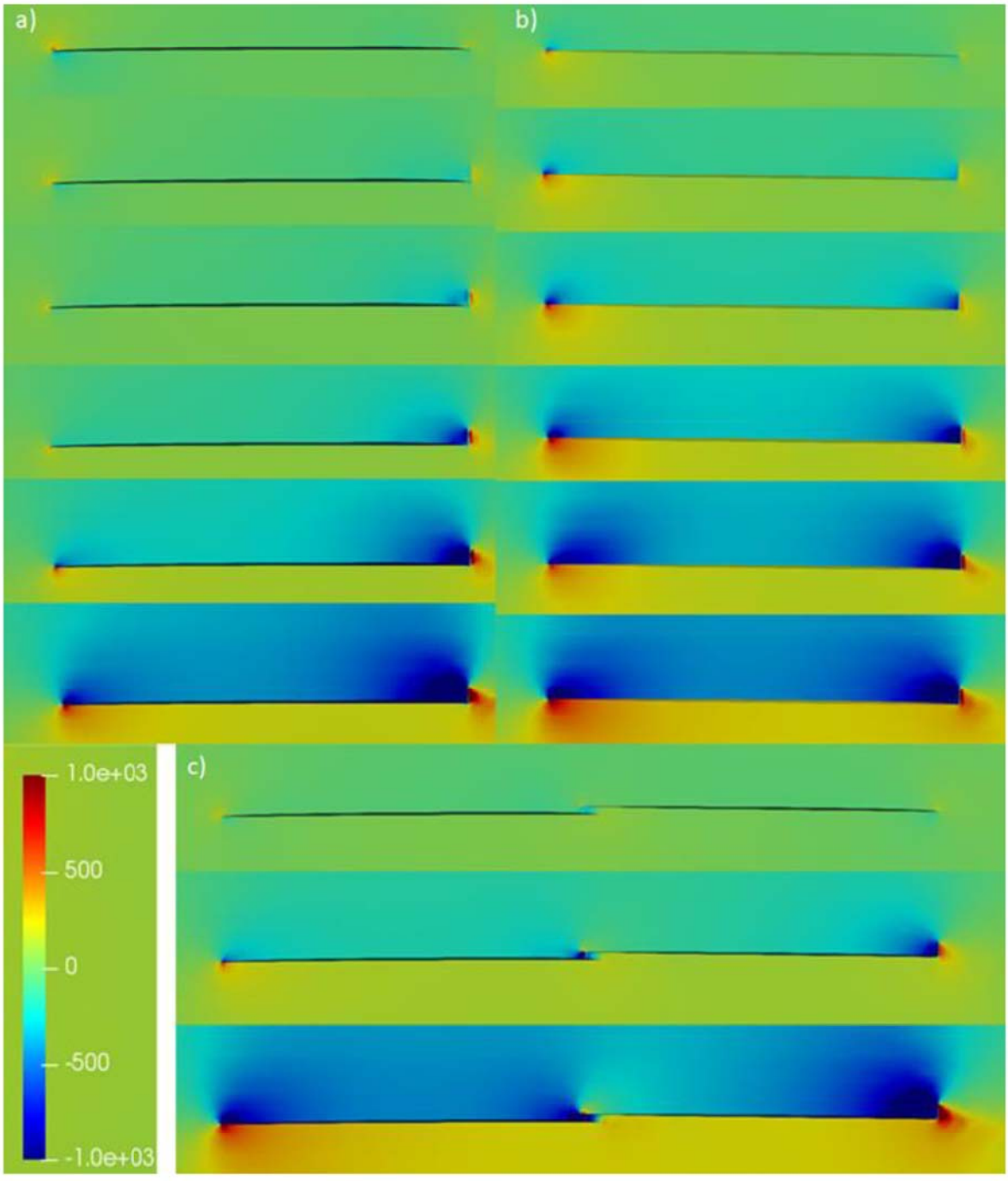

Fig. 4. Pressure profiles of airfoil with mid-chord Source along with pressure profiles of the airfoil sections No portion of the mid-chord Source extends above the leading edge of the trailing airfoil.

When evaluated independently, the leading-airfoil subsection has a negative lift at lower Source settings. This is due to free stream air impacting the upper surface and diverging from the lower surface. A trailing-edge Source on the leading-airfoil subsection is able to overwhelm the impact of free stream velocities because the Source intake forms lower pressures on an upper surface at $\alpha_P \approx 0°$; the lower-pressure air directly creates a strong lift force and indirectly extends forward to form a favorable leading-edge curl. The resulting ***L/D*** of the isolated leading section would continue to increase with increasing Source setting; however, the induced thrust is a force through a distance, which translates to a thermodynamic constraint of a reduced gain-loss ratio of reduced drag versus reduced Source thrust (i.e., increased Source ***Loss***).

The independently-evaluated trailing airfoil (Fig. 4b) has reasonable ***L/D*** based only on interaction with free stream velocities. Zero induced thrust is formed due to an $\alpha_P > 0°$. The upside potential of constantly increasing Source power is limited by $\alpha_P > 1°$ at the Source intake.

When leading and trailing airfoil sections are combined, there is a synergy where the higher lower-surface pressures created by the trailing airfoil section extend throughout lower surfaces (Fig. 4c), generating additional induced thrust on the lower surface of the leading airfoil. These results and thermodynamic constraints identify that *induced thrust created by a propulsor reduces drag and is able to cause very high L/D; however, the lower limit of L/D is regulated by power needs of the airframe at the intercept of Drag force (negative slope) with thrust slope (positive slope) to form the operating point for steady-level flight.* Designs and operational parameters of the airfoil and propulsor impact the shapes of the curves (see Fig. 5).

Hypothesis -.

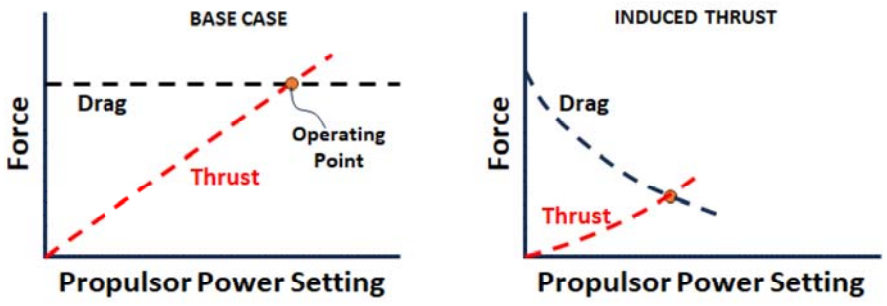

Fig. 5. Illustration of how induced thrust impacts force and power requirements. Graphs are at constant lift.

Figure 6 provides pressure profiles of the Fig. 5c sequence at additional Source settings. Tables 2 and 3 summarize the L/D of this airfoil sequence. At trailing Source settings of 0, 20, and 80 with 25% mid-chord power, the mid-chord Source airfoil has ***L/D*** of 4.97, 22.5, and 35.2, while the Fig. 7 airfoil has ***L/D*** of 8.5, 12.0, 31.7, and 36.7. This identifies that while working in concert, both Source terms are beneficial to the performance, but overall trends remain dominated by trailing-edge Sources in 2D simulations.

Table 2. Parameters for Fig. 4 airfoils.		
Mid-Chord Source Setting (m^4/s^2)	**Trailing Source Setting (m^4/s^2)**	**L/D**
Lead Airfoil, Fig. 4a		
N/A	1	-1.49
N/A	5	5.36
N/A	10	11.0
N/A	20	20.0
N/A	40	33.3
N/A	80	49.4
Trailing Airfoil, Fig. 4b		
N/A	1	10.5
N/A	5	19.1
N/A	10	25.1
N/A	20	33.2
N/A	40	39.6
N/A	80	41.5
Airfoil Sequence, Fig. 4c		
0	0	4.97
5	20	22.5
20	80	35.3

Table 3. Parameters for Fig. 4 airfoils.				
Mid-Chord Source Setting (m^4/s^2)	**Trailing Source Setting (m^4/s^2)**	**C_l**	**C_d**	**L/D**
0	0	0.0735	0.0086	8.5;
20	0	0.0601	0.0050	12.0;
0	20	0.2914	0.0918	31.7
15	20	0.2722	0.0741	36.7.

The pressure profiles of Fig. 6 illustrate how the mid-chord Source improves performance. As compared to a control with Source terms off, a mid-chord Source power setting of 20 increases the ***L/D*** from 8.5 to 12.0 (Figs. 6a and 6b) with no trailing Source. The primary mechanism for increasing ***L/D*** is the decrease of drag by causing the transfer of leading-edge higher-pressure air away from the front edges. A secondary mechanism for increasing ***L/D*** is generating lower pressures above the leading section and higher pressures below the trailing section. Performance is dependent on the thickness and shape of the leading section of the trailing section to reduce the higher-pressure region

formed by the leading edge of the trailing section.

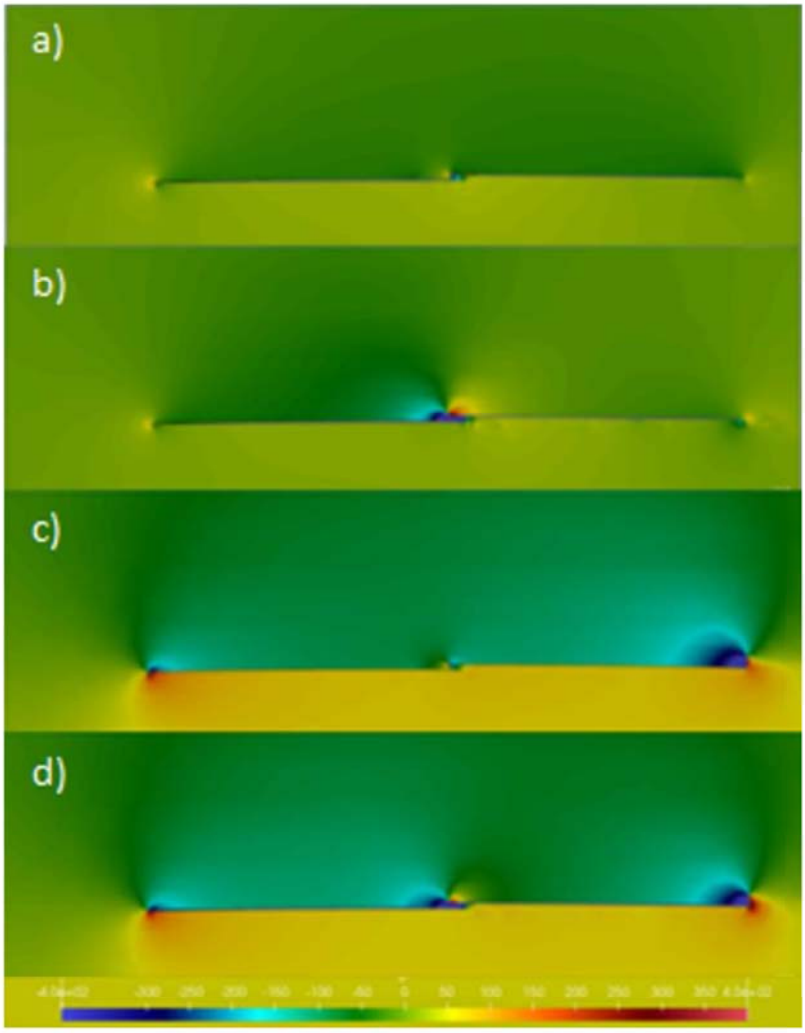

Fig. 6. Illustration of benefits of mid-chord Sources. For the 0.01 c airfoil the data of mid-chord Source

Use of a trailing Source (20 power setting) without the mid-chord Source increases ***L/D*** from 8.5 to 31.7. The trailing-edge Source improves the pressure profile throughout the airfoil with marked increases in ***L/D***, provided the surface before the trailing Source intake has $\alpha_P < 2°$. The trailing-edge Source decreases the magnitude of the higher-pressure region created by the mid-chord Source (Fig. 6b versus Fig. 6d).

The primary potential advantages of a mid-term Source are related to mitigating the impact of side-edge losses by a) mid-chord Sources replenishing lift forces and b) creating air flow patterns that beneficially change the vectors of side-edge air flows. Studies of these potential advantages cannot be evaluated in the 2D CFD simulations of this paper.

Discussion

A common Source of induced thrust is a low-pressure region on an upper surface having negative pitch. Induced thrust is present in essentially all high-performance airfoils (***L/D*** > ~40) without Sources as supported by the work of this paper for thin cambered airfoils and previous work on thicker airfoils. As a common feature on airfoils independent of any Source, induced thrust does not definitively correlate with lost thrust of a Source. However, when a Source induces thrust, there is ultimately a "transition" where induced thrust is only at the expense of similar and equal lost thrust by the Source. A gain-to-loss analysis considering the gain in L/D efficiency versus the loss in Source thrust provides a starting point for understanding this transition. Table 4 provides a summary of Propulsor-related heuristics based on the results and including useful equations for evaluating Source performance.

Table 4. Propulsion efficiency heuristics on designing to create aerodynamic lift and flight efficiency.

P-1. Loss of efficiency (lost work) correlates with: a) exit thrust velocity (u_e), b) angular-radial velocity, and c) temperature increase as ranked from highest to lowest losses for well-designed blades.
P-2. Exit thrust velocity may be used to estimate propulsor efficiency where $\eta_{prop} = [2\ u_0]/[u_e + u_0]$ under the assumption of effective blade design and mitigation of angular losses. In preliminary analysis, control airfoil boundary layers' velocities may be used as u_0. In general, propellers are more efficient that ducted jets due to larger pressure discs and respective lower u_e. Trends in jet engine design are for larger pressure discs (exit diameter) to provide lower u_e which is related to bypass ratios.
P-3. Angular losses tend to increase with increasing u_e, but may be corrected with: a) stationary vanes that convert angular velocity to thrust velocity, b) ducts that block radial dispersion of angular velocity, and c) pairing axially-aligned clockwise and counter-clockwise propellers.
P-4. Typical disc pressures may be estimated using wing loading (or planform loading with lifting body designs), ratio of pressure disc area to wing area, and L/D. L/D relates lift to thrust and pressure difference of the pressure disc, $\Delta P_S = [C_d/C_l * Weight / A_W] * A_W / A_S$ *for areas ("A") of the wing and propulsor*. At L/D=20 and A_W/A_P=15 pressures are: Military jets (2.33 kg/m^2, multiply by 9.8 to get Pa), commercial jets (1.7), commercial prop aircraft (0.66), prop drones (0.17), and HAPS/HALE (0.013).
P-5. For Lift Span technology, the pressure disc area is concentrated behind the Lift Span area, and so $\Delta P_{LS} = F\ \Delta P_W =$ where F = Planform area / Lift Span area. Due to this focusing of the propulsor pressures, distributed propulsion designs promoting induced thrust and lift inform designs toward narrower fuselages with more-focused lift pressures.
P-6. Pressure difference can be converted to velocity: **Force = 0.5 ρ A_P (u^2_e - u^2_0) = A_P ΔP** which can be specified to meet efficiency constraints per P-2.
P-7. The differential gain loss ratio for Sources is equal to $\left(\frac{\partial D}{\partial [Loss]}\right)_{Lift}$. This differential and its integral (i.e., the cumulative gain-loss ratio) can be determined using numerical integration of pressure and velocity profiles around a Source on an airfoil or wing.

Gain-to-Loss Ratio of Trailing-Edge Source - Gain-loss analyses of upper-surface trailing-edge Sources on airfoils are summarized by Figs. 7 and 8. At a constraint of constant lift, the gain is reduced drag forces. For the work of this paper, the loss is reduced thrust primarily caused by surfaces near the intake that choke air flow and reduce the velocity of discharged air.

Partial differential quantities were approximated by numerical analysis of a control volume around the Source in combination with ***L/D*** from CFD simulations. In flight, planes operate at constant lift, providing equation 6 as the relevant partial derivative for analysis:

$$\left(\frac{\partial D}{\partial [Loss]}\right)_{Lift} \tag{6}$$

As illustrated by Fig. 7, the partial derivative has maximum magnitudes as the power setting approaches zero. At lower power, the Source both reduces drag (i.e. converts drag to induced thrust) and increases lift. The Source creates lower pressures on surfaces afore the Source intake, a surface area referred to as the "Lift Span". Lower pressure on a Lift Span having surface of $\alpha_P < 0°$ of simultaneously increases the numerator and decreases the denominator of ***L/D*** for significant increases. As Source power increases, the airfoil's drag plateaus and the values of the partial derivative approach zero as shown in Fig. 7.

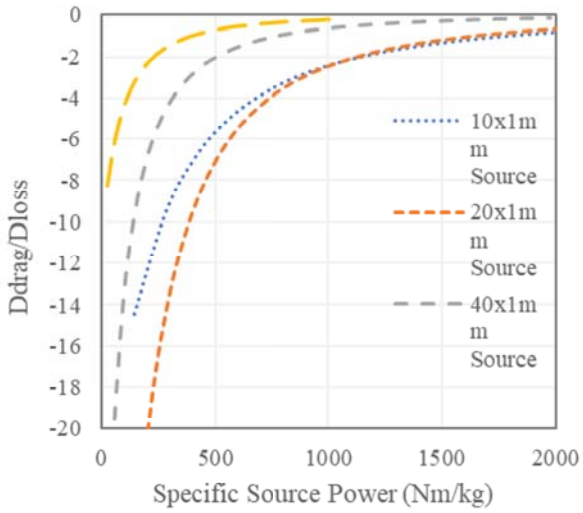

Fig. 7. Differential Gain-to-Loss ratio of power settings of trailing-edge Source of differing heights on a symmetric 0.01 camber airfoil at 0° pitch elliptic shape.

Figure 8 reports the numerical ingegrals of the partial derivativesas reported by Fig. 7. Typically, as the power of a properly configured trailing-edge Source increases, increasing amounts of power and energy are saved. The extent to which the power of the Source increases depends on the power needs of the entire airframe and the fraction of the total power provided by the respective trailing-edge Source. The Source of lost thrust is from choking of the intake due to decreasing pressures before the Source. The loss in Source thrust can be leveraged in excess of 10X at lower settings.

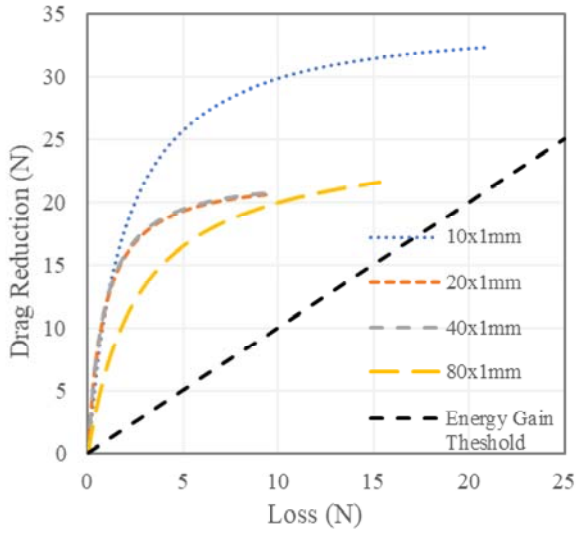

Fig. 8. Power savings due to reduced drag as Source power increases vs loss of the Source term.

Table 5. Propulsor Efficiency for Different Trail-Source Propulsors

Source Size	Source Setting (m^4/s^2)	C_d	C_l	$\Delta P / \rho$	V_{out}	η_P	L/D * η_P
10x1mm data	0	0.00775	0.074	-8	29.4		
	20	0.00845	0.340	1,532	59.4	**66.7%**	26.8
	40	0.00899	0.487	2,960	75.0	**56.8%**	30.7
	80	0.01087	0.693	5,704	96.2	**47.2%**	30.1
20x1mm data	0	0.00683	0.067	1	35.6		
	20	0.00700	0.245	958	50.5	**82.3%**	28.8
	40	0.00678	0.363	1,895	60.2	**74.0%**	39.6
	80	0.00642	0.536	3,745	74.1	**64.5%**	53.8
40x1mm data	0	0.00707	0.091	-2	37.6		
	20	0.00712	0.248	497	45.0	**90.7%**	31.6
	40	0.00683	0.370	994	50.8	**84.7%**	45.9
	80	0.00638	0.563	1,985	60.0	**76.7%**	67.7
80x1mm data	0	0.00684	0.081	2	39.2		0.0
	20	0.00695	0.191	267	43.0	**95.4%**	26.2
	40	0.00678	0.290	533	46.3	**91.6%**	39.1
	80	0.00615	0.463	1,064	51.9	**86.0%**	64.7

Table 5 summarizes the pressure and velocity data of Figure 8 and includes estimates of the equation of Heuristic P-2 on propulsor efficiency (η_P). The inlet velocity used for the P-2 equation is a representative average velocity of the boundary layer when the Source is turned off. A wing loading of 100 kg/m^2 was used as a reference. The data

show that larger propulsor areas lead to greater propulsor efficiencies, however, extending propulsors too high reduces efficiency due lower pressures on the Lift Span.

Mid-Chord Source versus Trailing-Edge Source

Figure 9 summarizes the separate ***L/D*** of the leading-airfoil section and the trailing-airfoil section with mid-chord and trailing-edge Sources for the Figure 6 sequence where the mid-chord Source is at 25% the power setting of the trailing edge Source. The constantly increasing induced thrust of the leading section results in constantly increasing ***L/D***. The ***L/D*** of the trailing section plateaus at a power setting of about 20, a value near 57° / 3°. This can be attributed to higher pressure region on the upper surface behind the mid-chord Source which increases while other areas of the surface have increasing lift pressures.

Figure 10 provides an insight for understanding the plateau of the ***L/D*** of the trailing section. A significant factor is large regions of $\alpha_P > 1$ for the greatest lift pressures; this leads to increasing drag with increased lift pressures. Interference, in the form of a high-pressure area behind the mid-chord Source, increases with increasing power; however, the adverse impact of the interference is not prevent continuously increasing overall L/D.

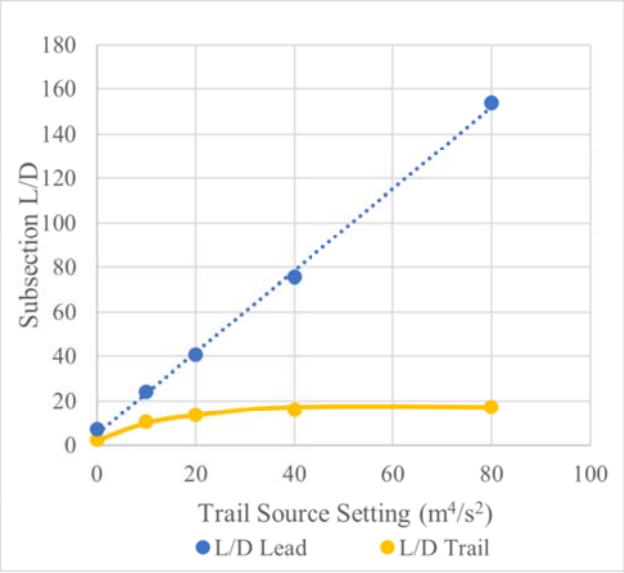

Fig. 9. L/D values for the leading-airfoil sections and trailing airfoil sections of Fig. 6.

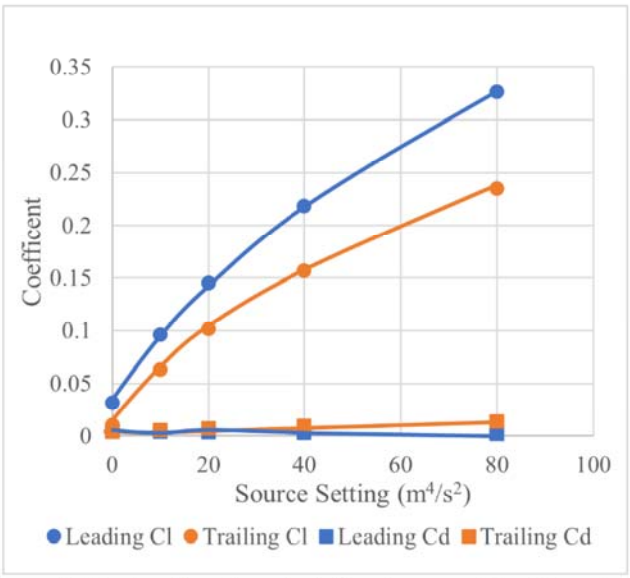

Fig 10. Lift and drag coefficients of leading-airfoil sections and trailing airfoil sections of Fig. 6.

Transforming Fuselage Drag to Lift

The ability to transform a leading-edge higher-pressure air into induced thrust is highly dependent on the shape and configuration of the airfoil. A key parameter in the specifying of the shape of the airfoil is t/c (thickness-chord ratio) with a high t/c needed for the body part of a blended-wing-body airframe. A high t/c leads to higher pitch Lift Spans afore a trailing edge Source.

Figure 11 illustrates airframes with thin center wings rather than high t/c fuselage bodies. As data of this paper reinforce, thin chamber center wings can have high L/D efficiencies and are compatible with direct use of bifacial panels as wing sections. [29-31] Applications like high altitude platform stations (HAPS) can have payload compartments small enough to be incorporated into fences rather than central fuselages. [32, 33]

HAPS use ultralight airframes, typically less than 5 kg/m^2, which are relatively fragile. Lower-aspect ratio aircraft can incorporate flexibility along the length with resulting robust designs while preserving ultra-light airframes.

The lower airframe of Figure 11 illustrates a narrow fuselage attached below a thin central wing. This design allows Sources to focus lift-generating lower pressures on a lower-span area that can be extended forward to maximize Source impact. Innovations and advances in science and engineering of this paper, and related papers, have a patent pending statuses that document invention dates. [34]

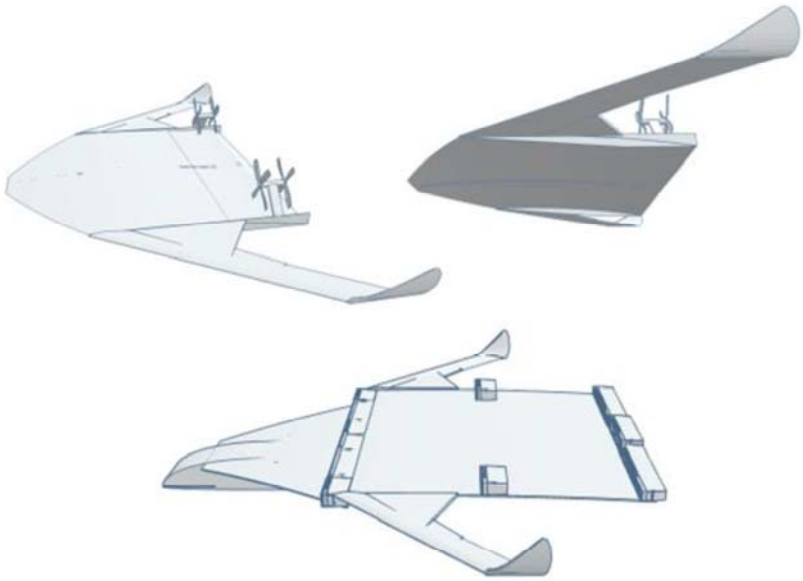

Fig 11. Illustration of modified blended-wing-body (BWB) aircraft configurations using thin-plate cambered airfoils enabling ultralight construction. Lower image illustrated distributed propulsion options and a narrow fuselage.

The next phase of this work is on 3D wing and airframes where the high **L/D * η_P** of Table 5 are trumped by the AR Equation (Equation 1). Fig. 12 summarizes preliminary wing (i.e., 3D) CFD simulations at 0.2 and 0.4 camber under several Source settings. At zero source settings, the L/D of these wings deviate from the AR Equation by less than 40%, being much closer to the AR equation than the 2D airfoil L/D values.

When the Source is inactive, the 0.04 camber has superior performance. This is a result of higher rates of lift generation from higher camber surfaces creating a more-favorable steady-state L/D.

As the trailing edge Source power increases, the 0.02 camber wing develops higher L/D. The average pitch of the Lift Span dominates performance as Source power increases.

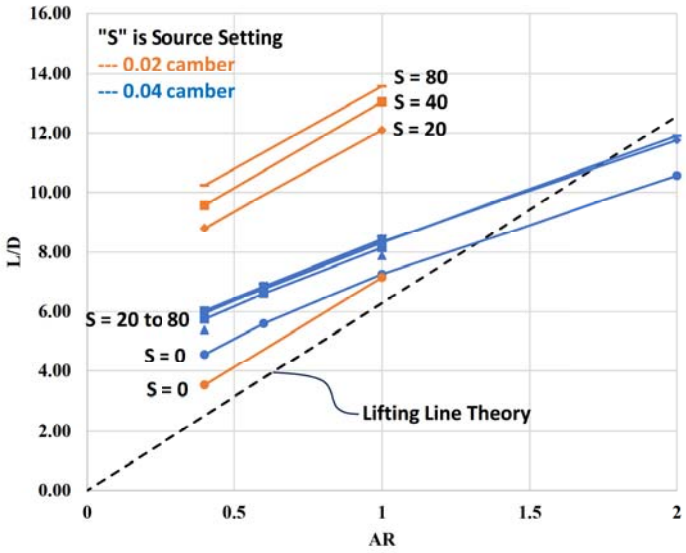

Fig. 12. Impact of trailing edge Sources on overcoming side-edge losses.

Fig. 13 illustrates a solution to this induced drag problem of higher-camber upper surfaces in the form of a raised Lift Span surface afore the trailing edge Source. The Lift Span pitch must be coordinated with the pitch of the nose and trailing section taper; the Lift Span pitch cannot be optimally adjusted by simply changing the pitch of the entire airframe. In the most-preferred configuration, the average Lift Span pitch will decrease with increasing Source power until the operating point of the aircraft is reached.

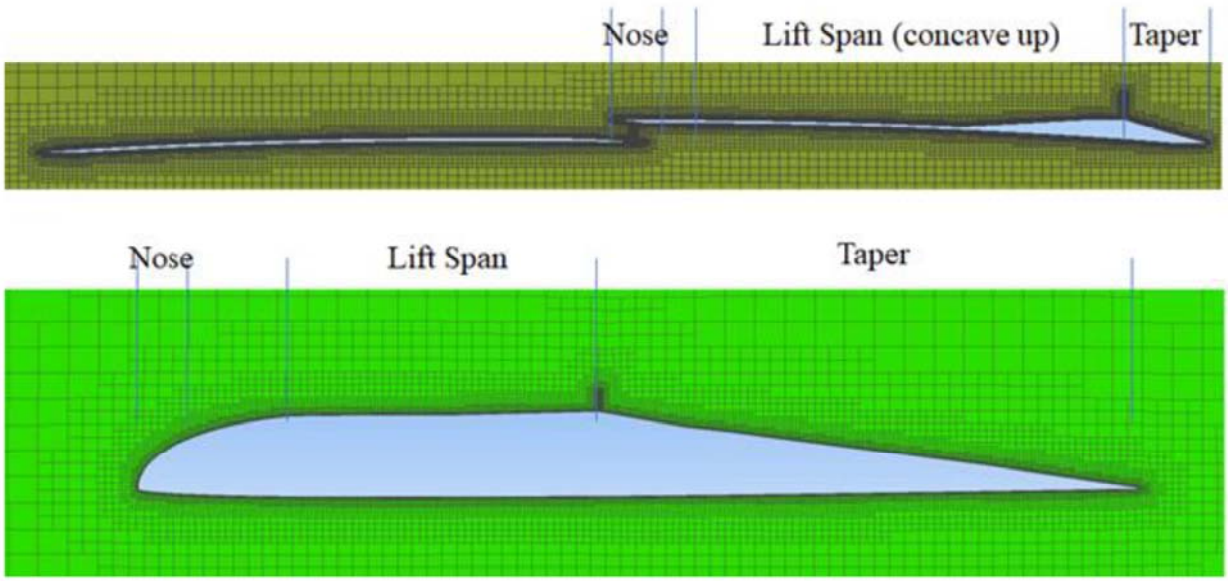

Fig. 13. Mesh image of fuselage airfoil illustrating three sections of partially decoupled design parameters for a flat Lift Span and a concave-upward Lift Span.

Interference between leading and trailing airfoil sections, such as illustrated by Fig. 13, have deterred pursuit of such configuration. However, rectangular nacelles on electric fans are considered to have performance advantages, especially in distributed propulsion. The implication is that the Fig. 13 crossover Source configuration has a very favorable gain-to-loss ratio with advantages of both ducted fan propulsion and extended surfaces for bifacial solar panels are considered.

Comparison to SUSAN

The benefit of trailing-edge Sources is typically associated with Boundary Layer Ingestion, itself associated with preventing flow separation which leads to a low pressure behind a fuselage or wing often associated with increased drag. [9-10] This paper identifies benefits of trailing edge Sources due to lift generation and induced thrust. This paper does not attempt to decouple boundary layer separation effects from the direct generation of pressures by Sources.

However, in the absence of gain-loss analysis on a Subsonic Single Aft Engine (SUSAN), increased choking of the engine intake could substantially offset the gain of reduced drag by producing higher pressures behind a fuselage centerline. Accordingly, claims of 30% increase in L/D-efficiency do not represent a complete analysis. Also, intake of a SUSAN centered behind a fuselage causes reduced pressure on the lower surface of the fuselage; an unnecessary expenditure of work which likely leads to loss. The instant research teaches toward locations of trailing edge engines where the low pressures of the intake are applied to upper surfaces of low α_P.

Conclusions

The flight efficiency of aircraft is a function of the pressure profile on the aircraft's surface and the efficiency of the propulsors. CFD simulations are able to generate the pressure profiles of airfoils and wing sections to both enable L/D to be estimated and provide insight into performance trends. The CFD simulations are also able to provide pressure and velocity profiles that identify if Source settings are reasonable and the gain-loss ratios associated with the interaction of Sources with surfaces. Results of these analyses on basic airfoil and wing sections are heuristic level summaries that are useful in aircraft design.

Distributed propulsion Sources ("Sources") are able to significantly increase the ***L/D*** of airframes. The primary mechanism for improving ***L/D*** is generation of lower pressures at the Source intakes; these lower pressures can improve the lift pressures throughout a 2D airfoil. Those same lower pressures are an artifact of choking the Source intake, which reduces thrust; however, lower Source setting can provide gain-loss magnitudes greater than 10.

The term "Lift Span" was defined in reference to the surface area afore a propulsor where pressures are reduced

by the Source intake. The gain-loss ratio was best for upper surface sources with Lift Span surfaces having average pitches <2°, with trailing section Sources on airfoils being the most effective and mid-chord Sources having application-specific benefits .

Side-edge losses significantly reduced the performance of thin cambered wing sections; however, Sources coupled with Lift Spans having decreasing pitch angles with increasing Source power were able to mitigate part of the side-edge losses in lift. Thin cambered wing sections are of particular interest since bifacial solar panels can be configured to be directly used as wing sections having solar productivity 2X to 3X the productivity of solar panels on Earth's surface. These higher productivities can be achieved without the greenfield or brownfield costs associated with solar farms on Earth's surface.

References

[1] Suppes, A., and Suppes, G., "Highly-Efficient Low-AR aerial vehicles in urban transit," *Proceedings of the 2014 Transportation Research Board Annual Meeting,* January, 2024, (see preprint http://www.terretrans.com/opensource.html).

[2] Suppes, G., and Adam, A., "Understanding Thin Cambered Airfoils and their Solar Aircraft Applications," *J. Aircraft,* Submitted for Review (see preprint http://www.terretrans.com/opensource.html).

[3] "Lifting-line theory," 2023, see https://en.wikipedia.org/wiki/Lifting-line_theory .

[4] Abbots, I.H., von Doenhoff, A.E., "Theory of Wing Sections," Dover Books on Aerospace, New York, 1959,

[5] Theodorsen, T., "Theory of wing sections of arbitrary shape," 1933,

[6] Burgmann, S. Dannemann, J. & Schroder, W., "Time-resolved and volumetric PIV measurements of a transitional separation bubble on an SD7003 airfoil | SpringerLink," *Experiments in Fluids,* Vol. 44, 2007, pp. 609-622.

[7] Klose, B., Spedding, G., and Jacobs, G., "Direct numerical simulation of cambered airfoil aerodynamics at Re = 20,000," 2021,

[8] Michna, J., and Rogowski, K., "Numerical Study of the Effect of the Reynolds Number and the Turbulence Intensity on the Performance of the NACA 0018 Airfoil at the Low Reynolds Number Regime," *Processes,* Vol. 10, 2022, pp. 1004.

[9] Mirhashemi, A., Chapman, J.W., Miller, C.J., "Tail-mounted engine Architecture and Design for the Subsonic Single Aft Engine Electrofan Aircraft," San Diego, CA,

[10] Jansen, R.H., Kiris, C.C., Chau, T., "Subsonic Single Aft Engine (SUSAN) Transport Aircraft Concept and Trade Space Exploration," San Diego, California,

[11] Russo, O., "Computational Fluid Dynamics analyses of a wing with distributed electric propulsion," 2022,

[12] Serrano, J., Tiseira, A., García-Cuevas, L., "Computational Study of the Propeller Position Effects in Wing-Mounted, Distributed Electric Propulsion with Boundary Layer Ingestion in a 25 kg Remotely Piloted Aircraft," *Drones,* Vol. 5, 2021, pp. 56.

[13] Osei, Emmanuel Yeboah, Opoku, Richard, Sunnu, Albert K. Adaramola, Muyiwa S., "Development of High Performance Airfoils for Application in Small Wind Turbine Power Generation," *Journal of Energy,* Vol. 2020, 2020,

[14] Lee, D., Nonomura, T., Oyama, A., "Comparison of Numerical Methods Evaluating Airfoil Aerodynamic Characteristics at Low Reynolds Number," *Journal of Aircraft,* Vol. 52, 2015, pp. 296-306.

[15] Achour, G., Sung, W., Pinon, O., "Development of a Conditional Generative Adversarial Network for Airfoil Shape Optimization," 2020-01-06,

[16] Wu, R., Soutis, C., Zhong, S., "A morphing aerofoil with highly controllable aerodynamic performance," *The Aeronautical Journal,* Vol. 121, 2016, pp. 1-19.

[17] Felder, J., Brown, G., DaeKim, H., "Turboelectric Distributed Propulsion in a Hybrid Wing Body Aircraft," 12 September 2011,

[18] Gohardani, A., Doulgeris, G., and Singh, R., "Challenges of future aircraft propulsion: A review of distributed propulsion technology and its potential application for the all electric commercial aircraft," *Progress in Aerospace Sciences,* Vol. 47, 2011, pp. 369-391.

[19] Pascual, B. R., Vos, R., "The Effect of Engine Location on the Aerodynamic Efficiency of a Flying-V Aircraft | AIAA SciTech Forum," 2020,

[20] Snyder, M.H., Zumwalt, G.W., "Effects of wingtip-mounted propellers on wing lift and induced drag. | Journal of Aircraft," *J. Aircraft,* Vol. 6, No. 5, 1969, pp. 392-397.

[21] Erhard, R., Clarke, M., and Alonso, J., "A Low-Cost Aero-Propulsive Analysis of Distributed Electric Propulsion Aircraft," January 11, 2021,

[22] Cunningham, M., Nigam, N., Ayyalasomayajula, S., "Integrated Vehicle-Propulsion-Control Design Architecture for Distributed Electric Propulsion-Enabled Aircraft," 2022-06-27,

[23] Loth, J., Loth, F., "Induced drag reduction with wing tip mounted propellers | Fluid Dynamics and Co-located Conferences," *AIAA 2nd Applied Aerodynamics Conference,* August, 1984, pp. 1-8.

[24] Sinnige, T., van Arnhem, N., Stokkermans, T. C. A., Eitelberg, G., Veldhuis, L.M., "Wingtip-Mounted Propellers: Aerodynamic Analysis of Interaction Effects and Comparison with Conventional Layout | Journal of Aircraft," *J. Aircraft,* Vol. 56, No. 1, 2019, pp. 295-312.

[25] Cole, J., Krebs, T., Barcelos, D., "Influence of Propeller Location, Diameter, and Rotation Direction on Aerodynamic Efficiency," *Journal of Aircraft,* Vol. 58, 2020, pp. 1-9.

[26] Krishna, Y.C., and Venkatesh, T.N., "Numerical investigation of aerodynamically efficient wing tip-mounted propeller configuration using coupled RANS–BEM approach," *Aircraft Engineering and Aerospace Technology,* Vol. 95, 2023,

[27] Kim, H.D., and Perry, AT, Ansell, PJ, "A Review of Distributed Electric Propulsion Concepts for Air Vehicle Technology," 2018.

[28] Zhang, X, Zhang, W., Li, W., Zhang, X., Lei, T., "Experimental research on aero-propulsion coupling characteristics of a distributed electric propulsion aircraft - ScienceDirect," *Chinese Journal of Aeronautics,* Vol. 36, No. 2, 2023, pp. 201-212.

[29] Deline, C., Palaez, S.A., Marion, B., "Bifacial PV System Performance: Separating Fact from Fiction," [online database]https://www.nrel.gov/docs/fy19osti/74090.pdf [cited Nov 27, 2023].

[30] "Albedo," 2023, see https://en.wikipedia.org/wiki/Albedo .

[31] Anonymous "Bifacial solar photovoltaics – A technology review - ScienceDirect,"

[32] Peck, A., "HAPS/HALE: Seeking Solar's Sweet Spot," *Inside Unmanned Systems,* 2020,

[33] say, G.B.H.y., "Airbus to spin-out Zephyr HAPS business as a separate company," [online database]https://www.datacenterdynamics.com/en/news/airbus-to-spin-out-zephyr-haps-business-as-a-seperate-company/ [cited Oct 24, 2023].

[34] Anonymous "Patent Portfolio," [online database]http://www.terretrans.com/tech.html [cited Jul 31, 2023].

Cover Letter

Galen Suppes, PhD
CEO
573-673-8164
gjsuppes@gmail.com

920 Beverly Rd
Apt 304
Charlottesville, VA 22911
https://hs-drone.com/

November 29, 2023

Dear Editor,

Please consider the attached paper entitled "Thermodynamic Analysis of Distributed Propulsion", for publication in Energy.

References in the paper refer to one of our papers in preprint and on under review. These references will be updated if the paper is accepted.

The contents of this paper are the result of a 4-year research path starting with fundamentals, and more recently, expanding to computational fluid dynamics. The 4-year and expanding patent portfolio is summarized at http://www.terretrans.com/tech.html.

A most-pertinent topic on **energy** is the use bifacial solar panels on thin cambered wings to produce power at 2X what is possible on Earth's surface. Preliminary economics identify payback periods of a few months, but there is a void of papers on the most pertinent topics to make this happen. A summary of what is possible is provide on our TRB Paper to be published in January, 2024. This work provides a foundation specific to the technology level of the readers of the Energy. The paper provides the start of a much-needed foundation for this burgeoning industry.

My ORCID ID is not maintained, but google scholars as an accounting of previous publications.

Sincerely,
/galen suppes/
Galen Suppes, CEO,
HS-Drone, LLC

Declaration of interests

☐The authors declare that they have no known competing financial interests or personal relationships that could have appeared to influence the work reported in this paper.

☒The authors declare the following financial interests/personal relationships which may be considered as potential competing interests:

Galen Suppes has patent #PCT/US20/36936 Multicopter with Improved Propulsor and Failsafe. pending to Suppes Family Trust. Galen Suppes has patent #CT/US21/16392 Flat Plate Airfoil Platform Vehicle. pending to Suppes Family Trust. Galen Suppes has patent #PCT/US22/14884 (addition of electric motor and new hybrid electric-fuel jet technology). pending to Suppes Family Trust. Galen Suppes has patent #5 more 2023 provisional applications pending pending to Suppes Family Trust. If there are other authors, they declare that they have no known competing financial interests or personal relationships that could have appeared to influence the work reported in this paper.